

# Neural signatures of different temporal-contextual structures embedded in episodic memory

Jiayu CHENG<sup>1,2</sup>, Ning SU<sup>1,4</sup>, Ruyi YAO<sup>1</sup>, and Sze Chai KWOK<sup>1,2,3,4\*</sup>

<sup>1</sup> Phylo-Cognition Laboratory, Division of Natural and Applied Sciences, Duke Kunshan University, Duke Institute for Brain Sciences, Kunshan 215316, China

<sup>2</sup> Department of Psychology, Academy of Advanced Interdisciplinary Studies, Wuhan University, Wuhan 430072, China

<sup>3</sup> Duke Kunshan University - The First People's Hospital of Kunshan Joint Brain Sciences Laboratory, Kunshan 215300, China

<sup>4</sup> Shanghai Key Laboratory of Brain Functional Genomics, Key Laboratory of Brain Functional Genomics (Ministry of Education), School of Psychology and Cognitive Science, East China Normal University, Shanghai 200062, China

✉ E-mail for Corresponding author: sze-chai.kwok@st-hughes.oxon.org



昆山杜克大学  
DUKE KUNSHAN  
UNIVERSITY



## Abstract

**Objective** Temporal memory, the ability to integrate events occurring at different time points along with their order, constitutes a fundamental component of episodic memory function. This study investigates how temporal memory is shaped by the macro-temporal context and the age of memories of encoded events, focusing on the variations in temporal distance and event structure and its underlying neural representations. **Methods** We recorded stereotactic EEG (sEEG) from 9 epilepsy patients during a three-day temporal order judgement (TOJ) task. On Days 1 and 2, participants encoded five videos per day (each with two distinct clips, repeated five times), followed by a TOJ test using frame pairs from the same day's clips. On Day 3, TOJ trials used frame pairs drawn from all 20 previously viewed clips. This yielded four trial types varying in contextual gap: within-video, across-videos within Day1, across-video within Day2, and across-day videos. Each pair was assigned a clip-based temporal distance (range 1–19). Generalized linear models (GLMs) were used to assess how trial type and temporal distance predicted TOJ accuracy. Neural analyses centered on ripple-derived peri-stimulus time histograms (PSTHs) aligned to stimulus, response, and inter-trial interval onsets. Cluster-based permutation tests were conducted to compare ripple rate between correct and incorrect trials. **Results** Participants showed above-chance TOJ accuracy on Day 3 (accuracy = 64.4%), which is significantly influenced by both trial type and temporal distance. GLM analysis reveals that greater temporal distance predicted higher accuracy ( $\beta = 0.16$ ,  $p < 0.001$ ,  $OR = 1.18$ ). At the level of temporal distance of within-video trials yielded the highest odds of correct responses ( $OR = 6.17$ ) compared to other trials of the same temporal distance, suggesting trial type is a strong predictor after controlling for temporal distance. Neural activity (ripples) time-locked to task events were analyzed in 8 patients. A significant increase in hippocampal activity during correct trials occurred 280 to 360 ms after the inter-trial interval (ITI) began. In the precuneus, correct trials showed significantly stronger stimulus-locked activity within 10 to 170 ms after stimulus onset. **Conclusion** These findings suggest that temporal order memory may depend on both macro-temporal context and temporal distance organization, with its neural implementation potentially occurring through early precuneus activity for stimulus processing and subsequent hippocampal ripples for consolidation.

**Keywords:** Temporal order judgment; Ripples; Temporal Distance; Hippocampus; Precuneus; iEEG

## Method

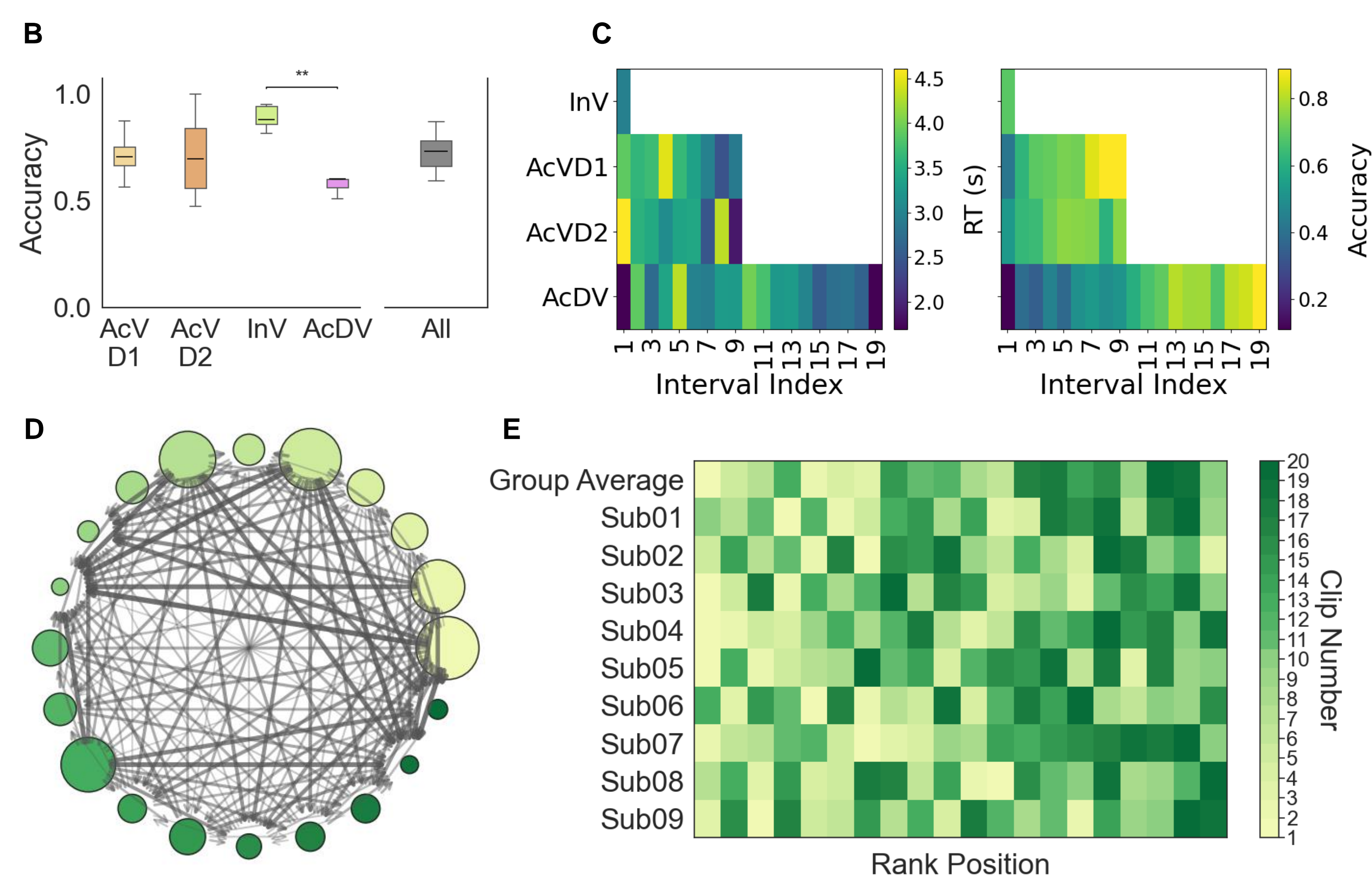
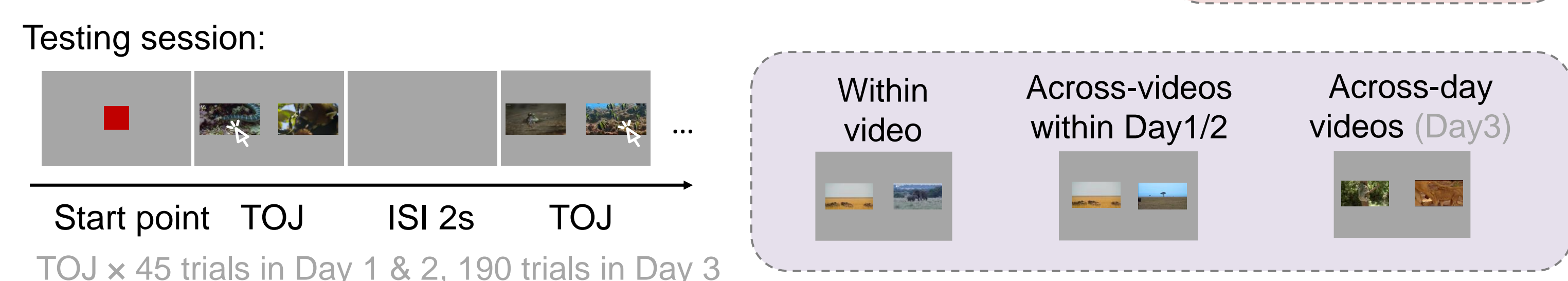
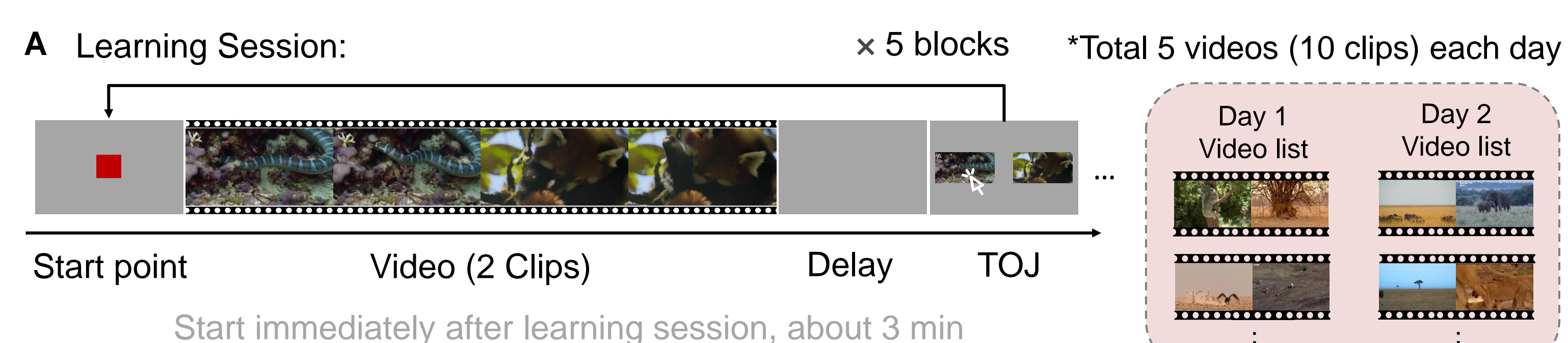


**Figure 1:** (A) Experimental structure. On Day 1 and Day2, participants encoded five videos per day (each with two distinct clips, repeated five times), followed by a TOJ test using frame pairs from the same day's clips. On Day 3, TOJ trials used frame pairs drawn from all 20 previously viewed clips. This yielded four trial types varying in contextual difference: within-video (InV), across-videos within Day1 (AcVD1), across-video within Day2 (AcVD2), and across-day videos (AcDV). (B) Accuracy across four different trial types (InV, AcVD1, AcVD2, and AcDV) and overall trials. The one-way ANOVA revealed a significant difference in accuracy only between within-video and across-day videos trials ( $p = 0.027$ ). (C) Heatmaps of participants' reaction time (left) and accuracy (right) as a function of temporal distance under different trial types during the three-day testing phase, showing opposite trends. (D) Pairwise dominance network for Bradley-Terry model. Colored circles denote different clips (1–20), circle size reflects relative BT strength (larger = stronger), while thicker/darker arrows indicate a larger BT advantage  $|\Delta\theta|$  and point from stronger to weaker. (E) The heatmap of mental temporal rankings derived from the Bradley-Terry model. Color-coded mental temporal order distribution of clips that were responded to in the 3-day TOJ task for each participant. Rows correspond to the group average (top) and individual subjects (Sub01–Sub09), while columns represent the mental rank positions of clips from highest to lowest BT-estimated skill. The color encodes the clips (1–20), as indicated by the colorbar.

## Results

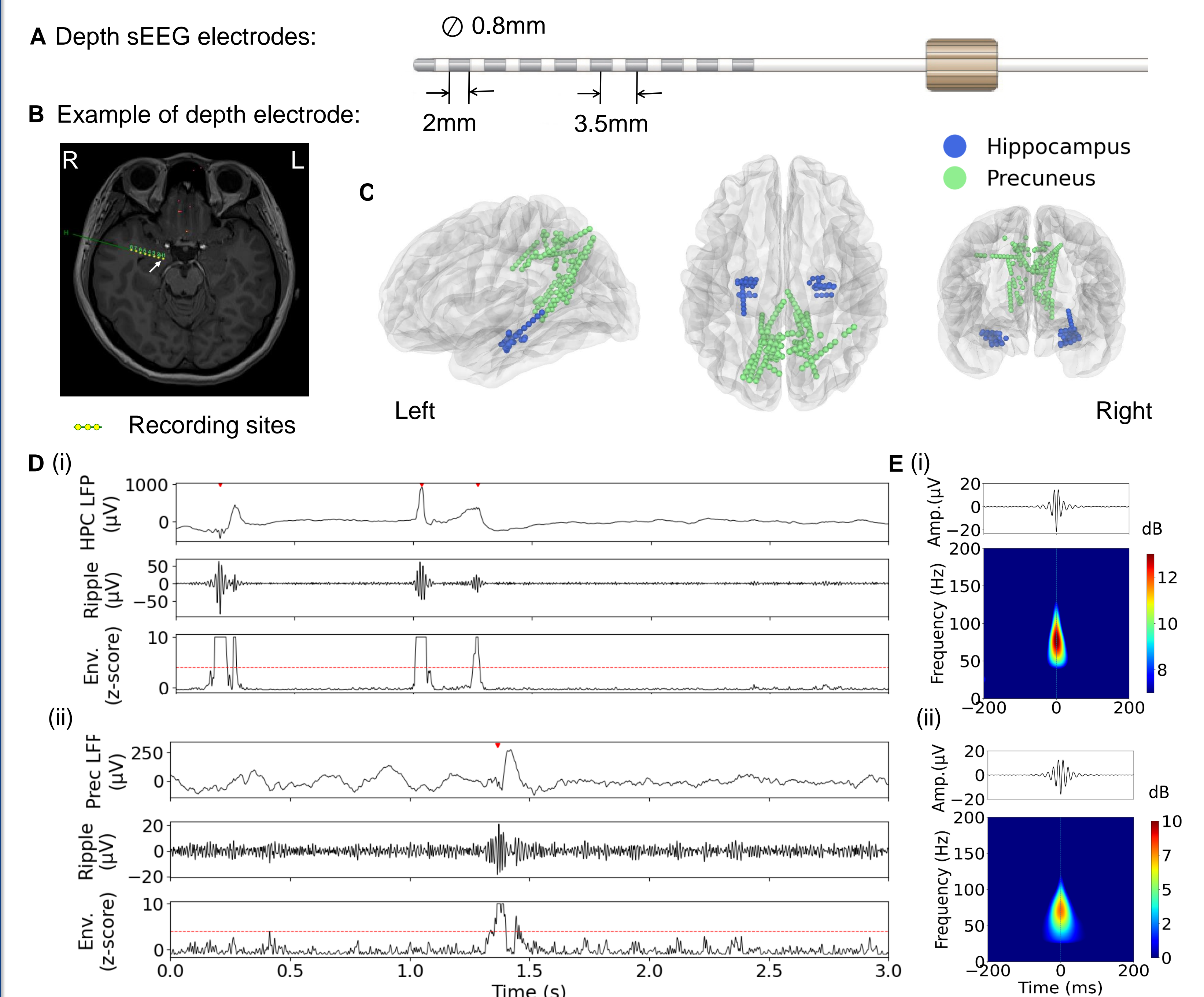


**Figure 2:** (A) Schematic diagram of depth iEEG electrodes used in our study. (B) Example of SWR events as they appear in the recordings. (C) The anatomical locations of recording sites located in Hippocampus (blue, total 20 contacts) and Precuneus (green, total 98 contacts). (D) From top to bottom: raw LFP; its ripple-band filtered component (70–180 Hz); and the normalized envelope of this component (z-score  $\geq 3$ ) used for ripple detection. (i) Hippocampus; (ii) Precuneus. (E) Grand average ripple-band (70–180 Hz) LFP (top) and corresponding power spectra (bottom) averaged across ripple events. (i) Hippocampus—7,394 ripple events from 8 patients across 49 channels. (ii) Precuneus—18,013 ripple events from 6 patients across 153 channels.

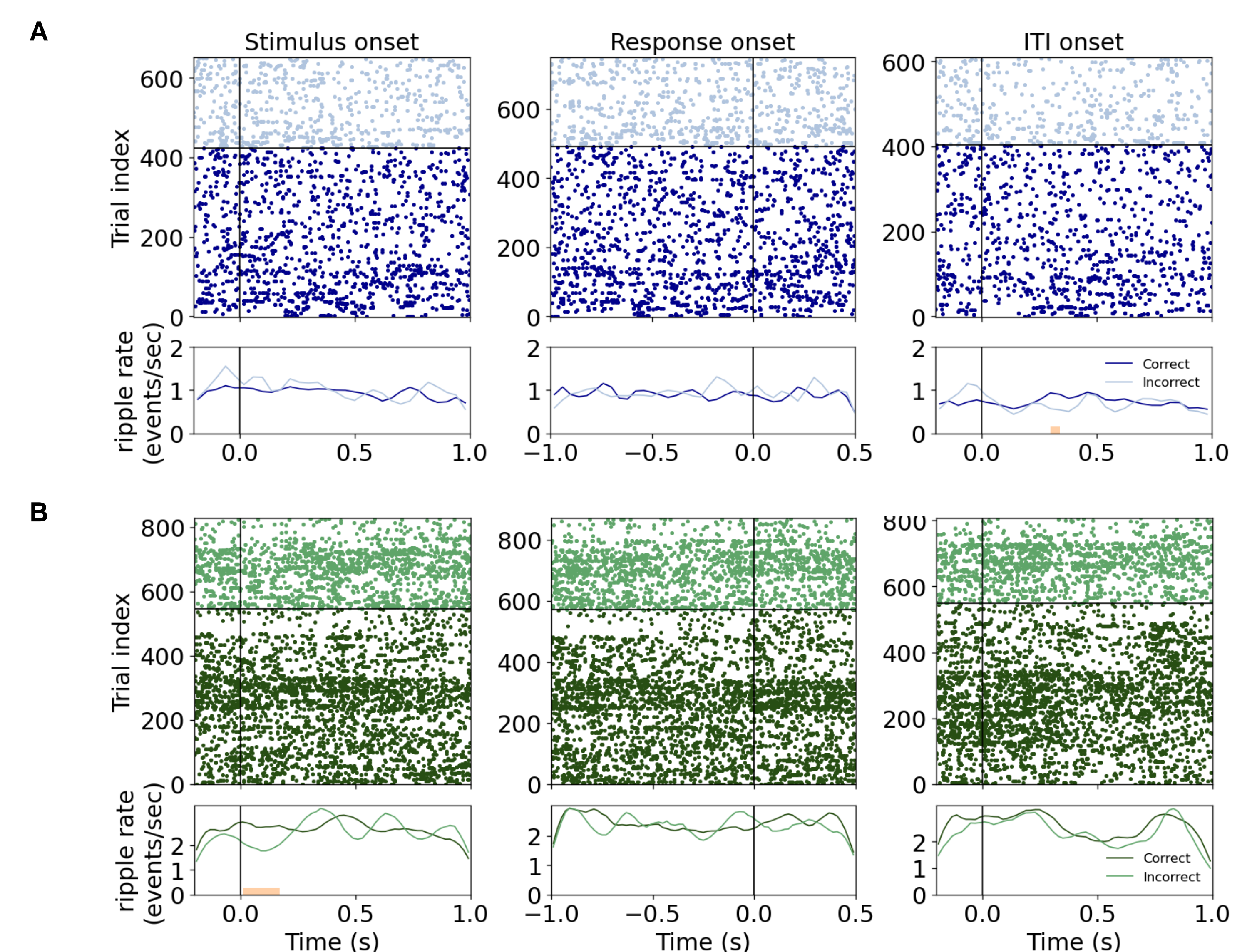


**Figure 3:** Ripple raster plot and PSTH time-locked to the onset of stimuli presentation, response, ITI ( $n = 8$  patients, 190 trials for each, Sub06 181 trials). (A) Hippocampus (ITI-locked PSTH): A cluster-based permutation test revealed a significant cluster at 280 ms to 360 ms (two-sided, cluster level,  $p = 0.030$ ), with correct trials showing stronger ripple activity than incorrect trials. (B) Precuneus (stimulus-locked PSTH): A cluster-based permutation test identified a significant cluster at 10 ms to 170 ms (two-sided, cluster level,  $p = 0.034$ ), with correct trials exhibiting greater ripple activity than incorrect trials. Orange bars mark significant time bins.

## Highlights

- Macro-temporal context and temporal distance jointly shape temporal order memory performance.
- Successful temporal memory relies on early precuneus engagement coupled with enhanced hippocampal ripple activity during consolidation.

We gratefully acknowledge the invaluable support of our collaborating medical team in the provision and collection of data for this study.